

Electron diffraction and Raman scattering evidence of a symmetry breaking at the metal-insulator transition of NdNiO₃

M. Zaghrioui,¹ A. Bulou,¹ P. Lacorre,² and P. Laffez^{1,*}

¹Laboratoire de Physique de l'Etat Condensé, UMR-CNRS 6087, Avenue O. Messiaen, 72085 Le Mans, France

²Laboratoire des Fluorures, UMR-CNRS 6010 Université du Maine, Avenue Olivier Messiaen, 72085 Le Mans cedex 9, France

(Received 24 April 2001; published 8 August 2001)

NdNiO₃ is studied by electron diffraction and by Raman scattering, and drastic changes are observed at the metal-insulator transition. These features are explained in the framework of a charge disproportionation of nickel, which is at variance from earlier results, but consistent with recent studies on smaller rare earth nickelates. The Raman spectra in the insulator phase are discussed with respect to the elpasolite arrangement. It is shown that several frequencies directly probe the charge transfer, which leads us to conclude that this parameter evolves over about 50 K below the transition.

DOI: 10.1103/PhysRevB.64.081102

PACS number(s): 71.30.+h, 61.66.Fn, 64.70.Kb, 78.30.Hv

Since the discovery of metal-insulator (M-I) transition in RNiO₃ perovskites ($R = \text{Pr, Nd, Sm, Eu}$),¹ many studies have focused on its origin. Using the classification developed by Zaanen, Sawatsky, and Allen, Torrance *et al.* have shown that these compounds are in the vicinity of the boundary between “low- Δ metal” and “charge-transfer insulator.”² The conduction was thus thought to arise from electron transfers between Ni3d and O2p orbitals. The transition was attributed to an electronic localization accompanied by an increase of Ni-O bond without any symmetry change. To date, the structure of these rare-earth nickelates was thought to be orthorhombic (space group $Pbnm$)³ in both the metallic (high temperature) and the insulator regimes (low temperature). However, a recent study of RNiO₃ with the smallest R (Ho, Y, Er, Tm, Yb and Lu) in the insulator phase by synchrotron x-ray and neutron powder diffraction revealed a monoclinic distortion (space group $P2_1/n$).⁴⁻⁶ This arrangement implies two independent Ni positions and the presence of a charge disproportionation ($2\text{Ni}^{3+} \rightarrow \text{Ni}^{3+\delta} + \text{Ni}^{3-\delta}$) in the insulating regime, while nickel is uniformly trivalent in the metallic regime. The existence of such a charge disproportionation in the lighter rare-earth nickelates has been questioned, and, if any, was considered to be very hard to detect.⁶ In this paper we show, by electron diffraction and Raman scattering, that such a symmetry breaking does also exist in NdNiO₃, and thus most probably in the whole rare-earth series of perovskite nickelates. In addition, the present study provides a way to probe the charge disproportionation.

Electron diffraction (ED) was performed on a ceramic sample synthesized with the process described in Ref. 1. Patterns were recorded on a Jeol 2010 transmission electron microscope (200 kV) fitted with a cooling sample holder working at liquid nitrogen (Gatan). The Raman spectra were performed on a NdNiO₃ thin film (about 0.15 μm thickness), grown on Si (100) by RF magnetron sputtering at 600°C and subsequent annealing under oxygen pressure (190 bar) at 800°C for 2 days. X-ray analysis reveals a highly textured material.⁷ Resistivity measurements show that the M-I transition occurs at 210 K upon heating (see Refs. 7-9 for more details). Raman spectra were measured with a T64000 spectrometer from Jobin-Yvon (multichannel with a cooled CCD

detector) in the triple subtractive configuration using a 600 μm grating. The incident wavelength was the 514.5 nm line of an argon-krypton laser with about 50 mW on the sample; the scattered light was collected in the 90° geometry. Measurements were performed down to 40 K in a cryo-cooler, under vacuum.

The reconstruction of the complete reciprocal space from ED patterns is consistent with cell parameters $a = a_p\sqrt{2}$, $b = a_p\sqrt{2}$, $c = 2a_p$, where a_p refers to the cubic average perovskite cell. At room temperature, the limiting reflection conditions are: no condition for hkl , $k = 2n$ for $0kl$, and $h + l = 2n$ for $h0l$; this confirms the space group to be $Pbnm$, as previously reported.³ Figures 1(a) and 1(b) show ED patterns along the $[100]^*$ direction at room temperature and at 97 K, respectively. Extra reflections clearly emerge at the forbidden $(0kl)$ positions for k odd, which indicates a symmetry change within the same cell parameters set. The reconstruction of the low-temperature reciprocal space shows that the conditions limiting reflections for hkl and $h0l$ remain unchanged. This leads us to propose the $P2_1/n$ space group for the low-temperature phase, similar to the nickelates with small rare earths.⁴⁻⁶ These investigations also showed that the phase transition is reversible with a small hysteresis, in agreement with the resistivity and thermal studies. The same results have been observed on different grains and for different cooling and heating cycles.

Raman spectra at several temperatures are shown in Fig. 2. At the lowest temperatures, the lines are fairly intense and narrow, and important changes occur on heating through the M-I transition. The most prominent change are the following:

- (i) The very intense line in the low-frequency range (63 cm^{-1} at 60 K) softens and strongly decreases in intensity at the vicinity of the M-I transition temperature,
- (ii) The two lines at 300 and 320 cm^{-1} move towards each other and tend to merge at T_{MI} ,
- (iii) The intense lines located at 400 and 460 cm^{-1} shift toward the line at 430 cm^{-1} , and they strongly decrease in intensity,
- (iv) A band in the vicinity of 620 cm^{-1} (at 60 K) undergoes a strong broadening and shifts towards lower frequencies when the temperature increases.

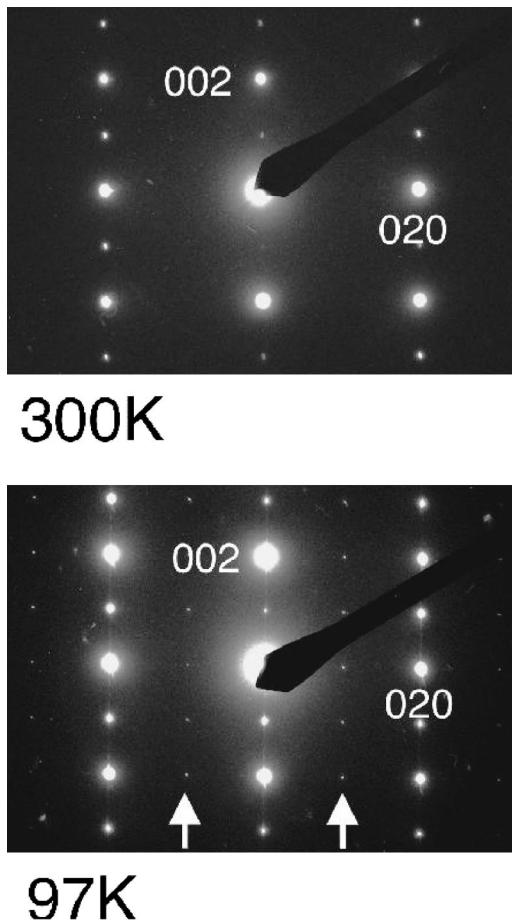


FIG. 1. Electron-diffraction patterns of the $[100]^*$ zone above and below the M-I transition. The arrows show the diffraction spots emerging below the transition, indexed by $(0kl)$ with k odd. Extra reflexions at $0k0$ and $00l$ with k and l odd are due to double diffraction.

The temperature dependence of the intensities of four of these lines (Fig. 3) and of the individual frequency shifts (Fig. 4) clearly show a singularity in the vicinity of 210 K. Some other lines also exhibit frequency discontinuity at T_{MI} (lines at 200, 300, and 400 cm^{-1}), but their intensity variations remain weak in both phases.

Therefore, both the ED and Raman scattering results give evidence for a symmetry breaking associated with the M-I transition. As shown below, these features are consistently explained as a consequence of a charge disproportionation of nickel ion, as found by Alonso *et al.* in heavy rare-earth nickelates. Below such a transition, two kinds of nickel ions ($\text{Ni}^{3+\delta}$ and $\text{Ni}^{3-\delta}$) and thus two kinds of Ni-O bond lengths are expected. This induces the loss of the b mirror of $Pbnm$ which uniquely leads to the $P2_1/n$ space group. Concerning the vibrational properties, 24 Raman-active modes are predicted in the $Pbnm$ space group ($7A_{1g} \oplus 7B_{1g} \oplus 5B_{2g} \oplus 5B_{3g}$). Only nine of them are intense enough to be observed (although some overlaps cannot be excluded). In the $P2_1/n$ space group $12A_g$ and $12B_g$ Raman active modes are predicted and it can be shown that they result from the $(7A_{1g} \oplus 5B_{3g})$ and $(7B_{1b} \oplus 5B_{2g})$ modes of $Pbnm$, respec-

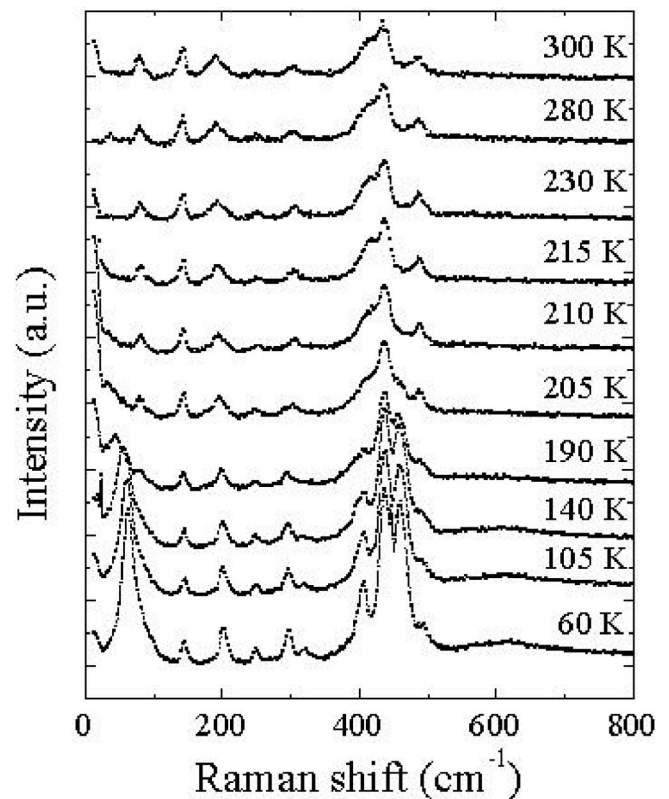


FIG. 2. Raman spectra of the NdNiO_3 thin film at several temperatures.

tively. Hence no extra lines are expected. The 14 lines observed below T_{MI} remain consistent with this monoclinic space group; however, this does not explain the observed drastic changes which, on the other hand, can be understood through the following analysis. The $P2_1/n$ space group can be obtained as derived from the cubic perovskite with first a $a^-a^-c^+$ octahedra rotation in Glazer's notation¹⁰ ($Pbnm$

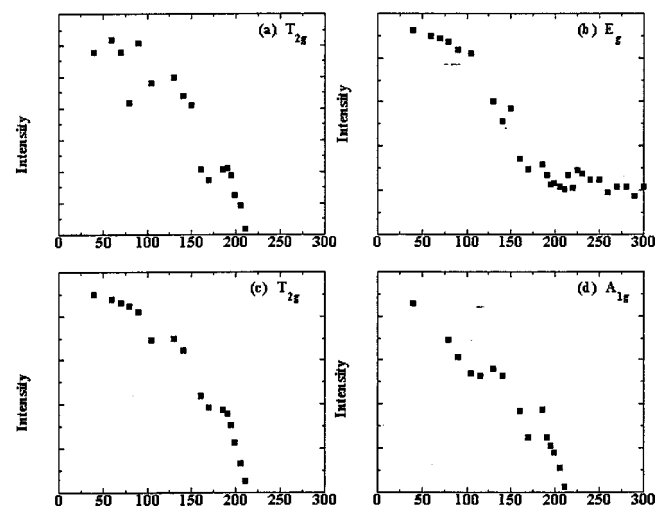


FIG. 3. Variation with temperature of the absolute intensity of the Raman modes located (at low temperature) around 63 (a), 320 (b), 460 (c), and 620 cm^{-1} (d). A_{1g} , E_g , and T_{2g} refer to the corresponding modes in an elpasolite structure (see text).

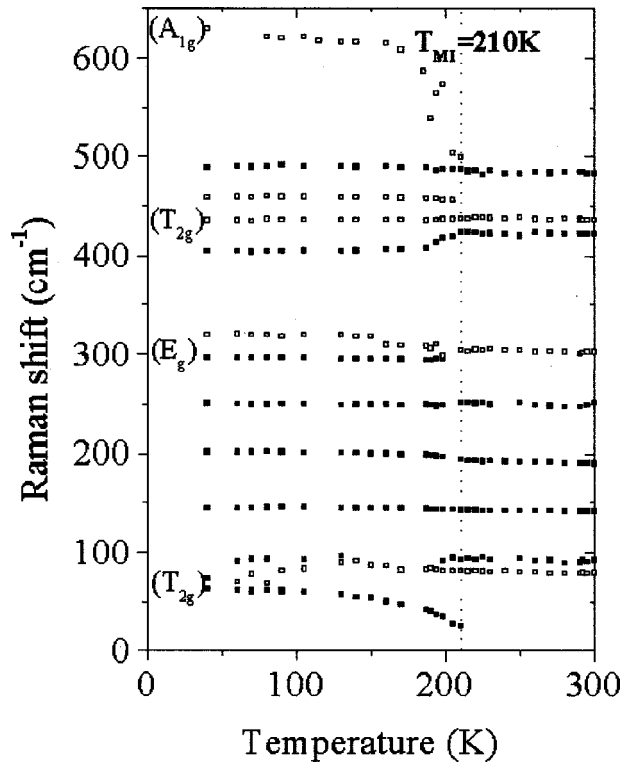


FIG. 4. Variation with temperature of the Raman shifts of NdNiO_3 . A_{1g} , E_g , and T_{2g} refer to the corresponding modes in an elpasolite structure (see text).

space group), and then a charge disproportionation (loss of b mirror). However, the same symmetry could also be obtained when the cubic perovskite first undergoes the charge disproportionation, and then, the octahedra rotation. The first step would be a cubic-perovskite/cubic-elpasolite phase transition (the elpasolite-type structure corresponds to the ordering of two cations with different charge and/or size in the perovskite octahedral sites). With regard to the resulting disproportionation of the bond polarizability, this (virtual) transition must give rise to stronger Raman signals than that for octahedra tilts alone (elpasolites are known to give rise to intense Raman signals). The Raman spectra of the low-temperature phase can hence be described mostly with respect to those of the cubic elpasolite, just perturbed by additional octahedra rotations. Four lines are predicted in the cubic elpasolite ($A_{1g} \oplus E_g \oplus 2T_{2g}$) and, according to Table I, their characteristics can be inferred from the phonon spectrum of the cubic perovskite (only modes becoming Raman active are considered here); Γ , X , M , and R refer to the $(0,0,0)$, $(1/2,0,0)$, $(1/2,1/2,0)$, and $(1/2,1/2,1/2)$ points of the cubic Brillouin zone, respectively. According to previous works^{11,12} they mainly consist of a low-frequency intense T_{2g} line (involving Nd displacements in NdNiO_3), a high-frequency intense A_{1g} octahedra breathing mode, and two medium frequency T_{2g} (intense) and E_g (weak) modes involving octahedra distortions (the three later modes can be considered as the internal modes of the free $\text{Ni}^{3+\delta}\text{O}_6$ octahedron). Hence, a transition by octahedra rotations from $Fm\bar{3}m$ to $P2_1/n$ gives rise to a triplet and a doublet in the frequency range of the

TABLE I. Compatibility relations between the Raman active modes of the rare-earth nickelates ($Pbnm$ and $P2_1/n$ space groups with o and m subscripts, respectively). (M , X , R refer to points of the Brillouin zone (see text). Mode of the cubic perovskite is $Pm\bar{3}m$, (c subscript). Mode of the cubic elpasolite is $Fm\bar{3}m$, (e subscript). The normal coordinates are given in Ref. 13 and part of the diagram is inferred from Ref. 14.

Fe ($Fm\bar{3}m$)	Rc ($Pm\bar{3}m$)	Γ_o ($Pbnm$) Fm ($P2_1/n$)	Xc ($Pm\bar{3}m$) Mc ($Pm\bar{3}m$)
A_{1g}	R_1	$7A_g$	$2X_1$
E_g	R_{12}	$12A_g$	$2X_2$
T_{1g}	R'_{15}	$5B_{3g}$	M_1
$2T_{2g}$	$2R'_{25}$	$7B_{1g}$	M_2
		$12B_g$	M_3
		$5B_{2g}$	M_4
			M_5

T_{2g} modes and E_g mode, respectively (Table I); all of them are already active in the $Pbnm$ symmetry phase (Table I) but, as explained above, they are expected to be enhanced thanks to the charge transfer. The experimental results are totally in agreement with such a scheme. The lines below 100 cm^{-1} and in the range $400\text{--}450 \text{ cm}^{-1}$ are attributed to the splitting of T_{2g} modes, while the doublet around 300 cm^{-1} results from the E_g mode. Such “multiplets” tend to collapse at T_{MI} and mostly, their intensities strongly decrease. These attributions are also supported by the calculation of the phonon spectrum in the cubic perovskite using a rigid-ion model.¹⁵ In the framework of the above description, the following additional comments and predictions can be done.

(i) The low-frequency mode that exhibits a soft behavior could have also been attributed to an octahedra liberation. This would be unexpected since octahedra has already undergone static rotations around the three axes (corresponding to modes R'_{15} and M_3 of the cubic perovskite). Only the $a^-a^-c^+ \rightarrow a^-b^-c^+$ octahedra tilts could be invoked, but this would be associated with the $P2_1/m$ space group,¹⁰ not consistent with the condition limiting reflections found by ED.

(ii) The line centred at 620 cm^{-1} at 40 K is attributed to the A_{1g} mode of the cubic elpasolite since this corresponds to the octahedron breathing, which usually exhibits the highest frequency among the g symmetry vibrations (i.e., the Raman-active modes in the present case). The effect of a charge transfer δ on the vibrational properties can qualitatively be deduced from previous works¹⁶ (PtCl chains with $\text{Pt}^{3+\delta}/\text{Pt}^{3-\delta}$): an increase of δ gives rise to an increase of the $\text{Ni}^{3+\delta}\text{-O}$ interaction greater than the decrease of the $\text{Ni}^{3-\delta}\text{-O}$ one, so that the vibrational frequency, that depends on the sum, increases. An important consequence is that this vibration closely probes the charge disproportionation. The softening observed over a large temperature range (50 K) on approaching T_{MI} indicates a progressive decrease of δ ; its broad character and the strong broadening it undergoes suggests a disorder.

(iii) The transition of NdNiO_3 can be described in terms of an electronic or a structural instability. In the later case, a (secondary) order parameter can be the normal coordinates of a mode that becomes totally symmetric in the low symmetry phase, i.e., a mode with B_{3g} symmetry in the $Pbnm$ space group (see Table I). It appears that in addition to the M_5 distortion mode (at high frequency), only the modes characteristic of the cubic elpasolite can be invoked. Consistently, they are the most sensitive to the transition (Figs. 3, 4), which supports the attribution. To our knowledge, it is the first vibrational evidence for a perovskite-elpasolite phase transition.

To conclude, the present study of NdNiO_3 shows that the metal-insulator transition is associated with important changes of structural and vibrational characteristics. The electron diffraction patterns and the set of Raman singularities can consistently be described in the framework of the $Pbnm-P2_1/n$ phase transition resulting from the charge disproportionation of nickel. Here a symmetry breaking is identified in the large rare-earth perovskite nickelates. It now appears that the charge disproportionation is not limited to small rare-earth compounds, but is most probably present in

all $R\text{NiO}_3$ perovskites ($R \neq \text{La}$), thus giving a more coherent pattern along the whole rare-earth series. The attribution of the Raman lines is given on the basis of a distorted elpasolite structure. It shows that the frequency variations offer a sensitive approach to probe the transition mechanism in NdNiO_3 . There is no doubt that key information will be obtained from compared studies of all the rare-earth nickelates. More generally, electron diffraction and Raman spectroscopy appear to be alternate convenient ways to study transition effects in such cases where structural modifications are so faint that they are undetectable by x-ray and neutron diffraction, as it was the case for NdNiO_3 . It is worth noting that Raman scattering investigations of NdNiO_3 have become possible mainly thanks to the availability of thin films, prepared by sputtering,¹⁷ which offers very compact materials able to avoid any significant heating in spite of irradiance high enough to give a good signal-to-noise ratio.

This work was partly supported by the Région Pays de la Loire, the CNRS, the FEDER and the INTAS Project No. 970177. We thank Dr G. Banerjee for her help during this work.

*Corresponding author. Email address: patrick.laffez@univ-lemans.fr

¹Ph. Lacorre, J. B. Torrance, J. Pannetier, A. I. Nazzal, P. W. Wang, and T. C. Huang, *J. Solid State Chem.* **91**, 225 (1991).

²J. B. Torrance, Ph. Lacorre, C. Asavaroengchai, and R. M. Metzger, *Physica C* **182**, 351 (1991).

³J. L. Garcia-Munoz, J. Rodriguez-Carvajal, Ph. Lacorre, J. B. Torrance, *Phys. Rev. B* **46**, 4414 (1992).

⁴J. A. Alonso, M. J. Martinez-Lope, M. T. Casais, M. A. G. Aranda, and M. T. Fernandez-Diaz, *J. Am. Chem. Soc.* **121**, 4754 (1999).

⁵J. A. Alonso, J. L. Garcia-Munoz, M. T. Fernandez-Diaz, M. A. G. Aranda, M. J. Martinez-Lope, and M. T. Casais, *Phys. Rev. Lett.* **82**, 3871 (1999).

⁶J. A. Alonso, M. J. Martinez-Lope, M. T. Casais, J. L. Garcia-Munoz, and M. T. Fernandez-Diaz, *Phys. Rev. B* **61**, 1756 (2000).

⁷N. Boisard, M. Zaghrioui, J. Ricote, D. Chateigner, P. Laffez, and P. Lacorre, European Material Research Society 1999 Spring

Meeting, 1-4 June 1999, Strasbourg, France (oral communication).

⁸P. Laffez, M. Zaghrioui, R. Retoux, and Ph. Lacorre, *J. Magn. Mater.* **211**, 111 (2000).

⁹P. Laffez, R. Retoux, P. Boullay, M. Zaghrioui, P. Lacorre, and G. Vantandello, *Eur. Phys. J.: Appl. Phys.* **12**, 55 (2000).

¹⁰A. M. Glazer, *Acta Crystallogr., Sect. A: Cryst. Phys., Diffr., Theor. Gen. Crystallogr.* **31**, 756 (1975).

¹¹M. Liegeois-Duyckaert, and P. Tarte, *Spectrochim. Acta, Part A* **30**, 1771 (1974).

¹²G. Baldinozzi, Ph. Sciau, and A. Bulou, *J. Phys.: Condens. Matter* **7**, 8109 (1995).

¹³R. A. Cowley, *Phys. Rev.* **134**, 4A 981 (1964).

¹⁴Ph. Daniel, M. Rousseau, A. Desert, A. Ratuszna, and F. Ganot, *Phys. Rev. B* **51**, 12 337 (1995).

¹⁵M. Zaghrioui, A. Bulou, P. Laffez, P. Simon, and Ph. Lacorre (unpublished).

¹⁶A. Bulou, R. J. Donohoe, and B. I. Swanson, *J. Phys.: Condens. Matter* **3**, 1709 (1991).

¹⁷Such films are now also obtained by laser ablation [G. Catalan, R. M. Bowman, and J. M. Gregg, *Phys. Rev. B* **62**, 7892 (2000)].